The influence of magnetic field gradients and boundaries on double layer formation in capacitively coupled plasmas

T. Schröder[1,2] O. Grulke[1,2] T. Klinger[1,2]

May 8, 2012

Abstract

The axial position of a magnetic field gradient has been varied for capacitive discharges in the linear plasma device VINETA. For low magnetic fields ($B \leq \mathcal{O}(10\ \mathrm{mT})$), double layers have been observed to form predominantly at the interface between the source and the plasma chamber. In particular, double layer position is independent of the position of the magnetic field gradient. However, shifting the axial location of the magnetic field gradient leads to a global change of the plasma potential and the strength of the double layer. For higher magnetic fields the position of the double layer can be disentangled from the position of both the diameter interchange and the magnetic field gradient.

1 INTRODUCTION

In astrophysical systems one has observed high energetic ion flows coming from e.g. the solar corona[1], the Aurora Borealis[2], or extragalactic jets[3]. One source of these fast ions has been identified as a spatially localized, steep gradient of the plasma potential, a so-called double layer (DL)[4]. A DL can easily be created in laboratory experiments by driving large currents through plasma[2,5,6]. However, DLs observed in space plasmas are usually current free. Although, a number of theoretical[7,8,9] and experimental[10,11,12,13,14,15,16,17] studies of these current-free DLs have been performed in the last decade, the exact formation mechanism is still under debate[18]. Nevertheless, applications such as ion thrusters[19,20,21] are already under development. The typical experimental approach is based on a device configuration including diverging magnetic fields[11]. Thereby, a magnetic field gradient (MFG) is generated in a fixed region between a small diameter plasma source region and an expansion chamber of larger diameter. Thus, the region of strong MFG is intrinsically correlated with the radial boundaries of the device, which is also the region where the DLs have been observed. Although it is not clear, what transition is triggering the DL formation, the MFG is typically taken as the important feature. Studies dealing with different magnetic field configurations are rare and they consider only little variations of the configuration at rather low magnetic field strength ($\approx 10 - 20$ mT)[13]. Others do not provide a plasma potential profile[17] or their kind of variations does not qualify to answer this specific question (e.g. varying the angle of B[20]). This paper presents results of experimental investigations on the relevance for DL formation of device geometry and magnetic field configuration. In contrast to previous studies the MFG position ($\Delta z_{MFG} < 60$ cm), the magnetic field strength ($18-72$ mT) and the position of the change of the vessel diameter (10 cm – 40 cm) are studied independently.

2 EXPERIMENTAL SETUP

The experiments have been carried out in the linear helicon device VINETA[22] illustrated in Fig. 1. The vacuum chamber is immersed into a set of 36 planar, water-cooled magnetic field coils. The coils can be positioned almost freely along z. They are powered individually allowing for a flexible shaping of the axial magnetic field. This includes the possibility to generate similar magnetic field gradients (MFG) at different

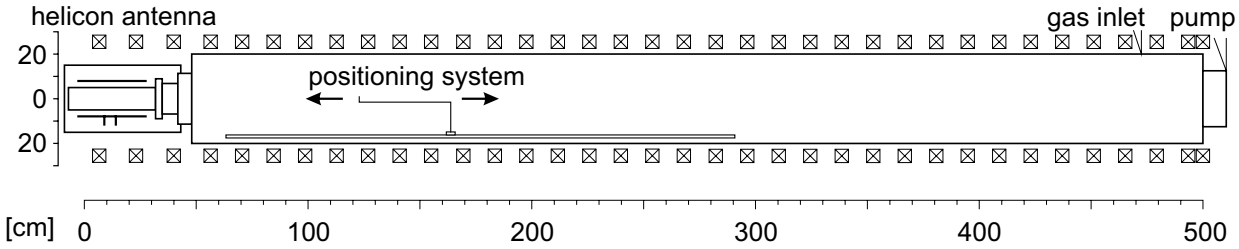

Figure 1: Sketch of the VINETA immersed in its magnetic field coils. The Langmuir probe (LP) and the emissive probe (EP) are installed on a z-table, being able to penetrate the source tube.

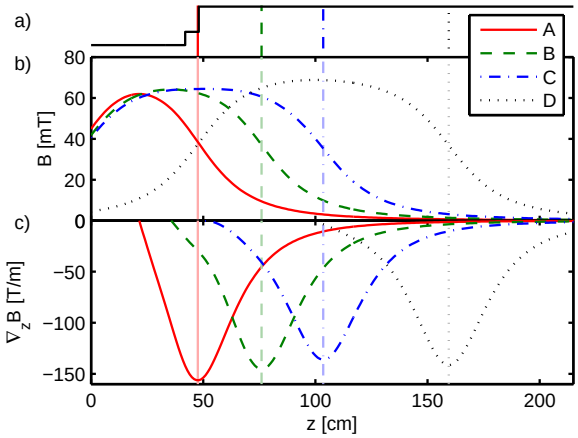

Figure 2: Different magnetic field configurations of the present study: a) Standard VINETA outline; b) magnetic field strength; c) magnetic field gradient. The vertical lines mark the position of the maximum absolute MFG, respectively. $z_A \approx 48$ cm, $z_B \approx 76$ cm, $z_C \approx 104$ cm, $z_D \approx 160$ cm

axial (z-)positions. For the present experiments four configurations are studied. The magnetic field strength for each configuration (A–D) and its respective axial derivative is depicted in Fig. 2.

Additionally, the geometry of the device can be altered, i.e. the device diameter with respect to the axial position z can be changed. Fig. 3 shows the three different setups used in this study.

The original setup (setup 1) is characterized by its source region. It consists of a Pyrex tube with a diameter of 10 cm surrounded by a water cooled

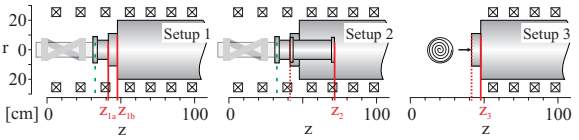

Figure 3: The three source types: Setup 1) $M = 1$ helicon double saddler setup Setup 2) "Setup 1" with an elongation of the small diameter section. Setup 3) Source displaced by a spiral antenna and source magnetic field coils removed.

standard $m = 1$ helicon antenna. The main chamber of the VINETA has a diameter of 40 cm. Due to the port connection (20 cm), setup 1 includes three regions of different diameter separated at the axial positions $z_{1a} \approx 42$ cm and $z_{1b} \approx 48$ cm. These positions are close to the MFG of configuration A.

Setup 2 differs from the original one by a 30 cm stainless steal tube. It extends the small diameter region of the source into the chamber. Thereby, the setup has only a single step in the diameter profile at $z_2 \approx 72$ cm. This step is located close to the MFG of configuration B.

For setup 3 the source has been replaced with a spiral antenna[23]. The new source diameter is 20 cm, which is twice the diameter of the original source. It is connected to the 40 cm diameter discharge chamber at $z_3 = 48$ cm.

Setup 1 and setup 2 will be operated at $P_{12} = 100$ W rf power for a capacitive Argon discharge[24] at a neutral gas pressure of $p_{12} = 0.03$ Pa. Setup 3 uses an inductively coupled plasma with an increased neutral

gas pressure ($p_3 = 0.05$ Pa) and rf power ($P_3 = 200$ W). For convenience, the combinations of magnetic field configurations (A–D) and setups (1–3) will be referred to as cases, e.g. case 1A refers to setup 1, configuration A.

Case 1A will be used to reproduce prior works[11,14,16,12,13,15,17], since the MFG is located close to the diameter change. Case 2B is quiet similar to case 1A, therefore, it is possible to study the influence of the distance to the source. If setup 1 and setup 2 are compared, one can study the influence of the geometry. By comparing the different configurations the impact of the MFG position on the DL can be qualified. Since in setup 3 the geometry effects are mostly suppressed, it will help to get a better understanding of the influence of the MFG. Finally, with setup 2 the influence of the magnetic field strength is studied. Therefore, the magnetic field strength is reduced by a factor of 4. This will change the gyroradii ($\propto B_z$), while the expansion of the plasma (MHD: $\propto B_{z0}/B_z$) remains the same.

A DL is characterized by its strength $\varsigma = e\Delta\Phi/(k_B T_e)$ and width $\lambda = \Delta z/\lambda_D$. Thereby, $\Delta\Phi$ is the potential difference over the axial distance Δz, T_e is the downstream electron temperature, and λ_D is the Debye length[2]. It leads to a local violation of quasi-neutrality and is not related to an ambipolar diffusion following the Boltzmann relation $n = n_0 \exp(e\Phi/k_B T_e)$. To analyse the DL formation the plasma potential profiles $\Phi(z)$ are measured using a strongly emitting emissive probe (EP)[25]. Additionally, electron density profiles $n_e(z)$ and electron temperatures T_e are measured by a rf compensated[26] Langmuir probe (LP). Both probes have been installed on a positioning system inside the vacuum vessel (cf. Fig. 1).

3 RESULTS

The measured axial profiles of the plasma potential and density for the different configurations are depicted in Fig. 4. The most important parameters are compiled in Tab. 1 and 2.

First, we consider case 1A and case 2B (Fig. 4a,b). In these cases both the diameter change and the MFG are located at the same position, which is comparable to prior publications[11,12,13,14,15,16,17]. Each case shows a potential drop close to the position of the maximum MFG as well as to the change of diameter between the source region and the expansion chamber. Plasma potential and density profiles do not follow the Boltzmann relation. Hence, both cases show a weak DL with $\varsigma = 2.1$ for case 1A and $\varsigma = 5.6$ for case 2B. In setup 2, where the distance between source and both transitions is larger, the plasma potential is generally much higher (by a factor of 2).

If the MFG is shifted into the vacuum chamber (i.e. away from the geometrical transition) the DL weakens (2C) and finally vanishes (1C). Instead, the plasma potential displays a linear run at the MFG associated with a density decrease following the Boltzmann relation. Comparing case 2C with case 2B, the DL structure of case 2C is found inside the small diameter extension at $z \approx 55$ cm. A similar shift of the DL structure however into opposite direction can be observed in case 2A, where the MFG is located between source and geometrical transition. The density profile displays the plasma expansion due to the MFG, whereas the potential drop occurs more than 30 cm in front of the tube. In particular, the position of the DL is neither close to the location of the MFG nor at the diameter change.

If the geometrical transition is absent as in setup 3 (Fig.4c), a substantial potential drop can be observed at the position of the MFG for case 3C. Nevertheless, if the density profile is taken into account, this drop is due to the widening of the plasma and not a DL. For a larger distance of the MFG to the source, this potential drop is getting smaller (case 3D). Experiments in setup 1 and 2 with comparable parameters ($p = 0.05$ Pa, $P = 200$ W) have shown DLs.

To investigate effects arising from the magnetic field strength, it is lowered for setup 2 by a factor of 4 (Fig.4d). If the MFG is located close to the geometrical transition the magnetic field strength has almost no influence on the plasma potential and density profile (case $2B_{1/4}$). However, if both transitions are not aligned (case $2A_{1/4}$), a weaker magnetic field nullifies the spatial shift of the DL observed in case 2A and the DL always forms at the geometrical transition regardless of the location of the MFG.

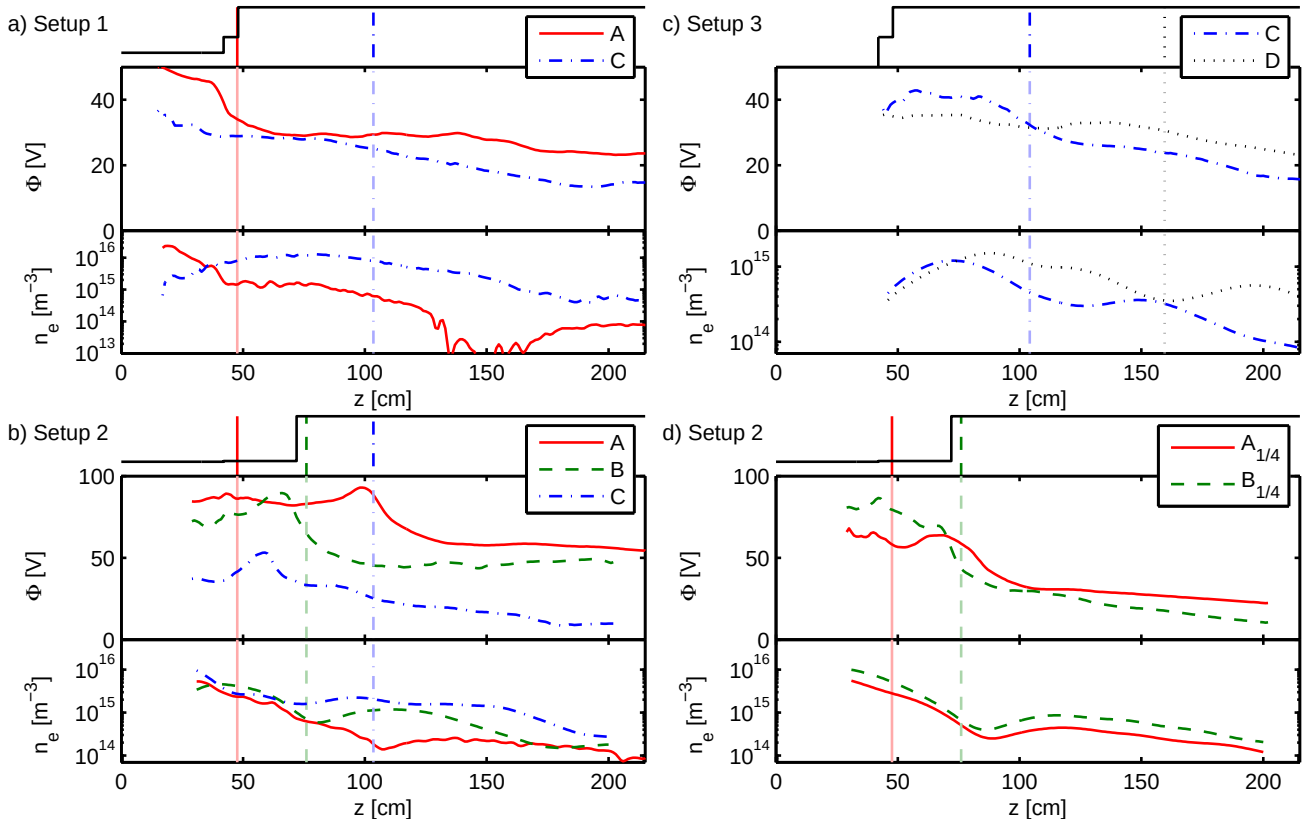

Figure 4: Experimental data for all considered cases. Each subfigure a)–d) consists of three parts, the geometrical outline of the setup, the plasma potential Φ, and the electron density n_e. The line styles correspond to the magnetic field configurations (A–D) given by Fig. 2. The vertical lines mark the position of the minimum MFG, respectively. Subfigure d) shows case 2A and 2B for a four times weaker magnetic field.

4 SUMMARY&CONCLUSIONS

The DL experiments done by other groups[11,12,13,14,15,16,17] have been successfully reproduced. The observed DLs are current-free in agreement with the theory given by Lieberman[27].For the typical setup with a MFG located at the position of the diameter change of the device, a DL has always been observed at the position of the MFG (1A, 2B, $2B_{1/4}$), which is also the position of the diameter change. The distance of the transitions to the source has a general effect on the magnitude of the plasma potential. Therefore, the distance influences the absolute potential drop of the DL but has no influence on its relative position. Numerical simulations suggest that the formation of a current-free DL is predominantly controlled by an increased loss of ions in the diverging magnetic field region of the MFG[8]. The present results demonstrate, the MFG position alone is not sufficient to form a DL (c.f. setup 3). In laboratory DLs form in combination with the right radial boundary conditions. According to case 1C, the MFG does not generate a DL unless it is located close to a geometrical transition. Apparently, these combinations are not limited to cases where MFG region and geometrical transition are aligned. As shown in case 2A, a DL can also form if

case	z_{edge} [cm]	Δz [cm]	$\Delta\Phi$ [V]	λ [1]	ς [1]
1A	38	8	16.5	345	3.3
1C	31	3	3.0	133	0.6
2A	102	13	34.0	91	6.8
2B	68	11	46.0	338	9.2
2C	60	6	20.5	189	4.1
$2A_{1/4}$	68	11	34.0	209	6.8
$2B_{1/4}$	69	8	40.0	133	8.0
3C	95	17	12.0	430	2.4
3D	77	15	4.5	484	0.9

Table 1: Characteristic parameters of the Plasma potential structures for different setups and configurations. Due to issues with the temperature measurements we can only assume an electron temperature of $T_e \approx 5$ eV.

case	n_e $[10^{14}\text{m}^{-3}]$	coll_e $[10^{-2}]$	col_i $[10^{-4}]$	mfp_e [cm]	mfp_i [cm]
1A	51.3	5.5	6.7	3.7	124.3
1C	54.1	7.1	8.6	3.6	124.1
2A	1.3	26.6	32.3	19.6	128.2
2B	26.1	4.9	6.0	6.2	126.2
2C	27.4	4.8	5.8	6.0	126.1
$2A_{1/4}$	10.0	23.3	28.3	11.0	127.5
$2B_{1/4}$	7.7	19.8	24.0	12.4	127.6
3C	17.7	8.7	10.6	6.5	76.5
3D	28.7	13.9	16.9	4.9	76.1

Table 2: Plasma density, collision-parameter (coll), and mean free paths (mfp) for electrons (e) and ions (i) at $z = z_{\text{edge}} + \Delta z$,
where $\text{coll} = \text{f}_{\text{coll}}/\text{f}_{\text{gyro}}$ and $T_e \approx 5$eV

the MFG is located upstream of the transition. In this case, for a low magnetic field, the DL forms close to the diameter change. For higher magnetic fields, its position is shifted further and further to the low field side. This indicates a threshold of the ion-gyroradius for DL formation. If this is the case, the dependency appears to be quiet complex and will need further investigation. Due to this study the parameters have the following effects on the DL formation:

1. **Position of the diameter change:** Determines predominantly the position of the DL.
2. **Magnetic field strength:** Determines the influence of the magnetic field configuration.
3. **Magnetic field gradient:** Supports DL formation if located close to diameter change. Its relative position to the position of the diameter change determines the relative position of the DL.
4. **Distance of the source:** Influences the global plasma potential. The closer the source, the higher the plasma potential and the higher the potential drop.

References

[1] R W Boswell. The current-free electric double layer in a coronal magnetic funnel. *Astrophys. J.*, 640(2):L199, 2006. doi:10.1086/503155.

[2] L Block. Double-layer review. *Astrophys. Space Sci.*, 55(1):59–83, 1978. doi:10.1007/BF00642580.

[3] J Borovsky. Parallel electric-fields in extragalactic jets - double-layers and anomalous resistivity in symbiotic relationships. *Astrophys. J.*, 306(2):451–465, 1986. doi:10.1086/164356.

[4] M Raadu. The physics of double-layers and their role in astrophysics. *Phys. Rep.*, 178(2):25–97, 1989. doi:10.1016/0370-1573(89)90109-9.

[5] P Coakley. Laboratory double-layers. *Phys. Fluids*, 22(6):1171–1181, 1979. doi:10.1063/1.862719.

[6] N Hershkowitz. Review of recent laboratory double-layer experiments. *Space Sci. Rev.*, 41(3-4):351–391, 1985. doi:10.1007/BF00190655.

[7] F Perkins. Double-layers without current. *Phys. Rev. Lett.*, 46(2):115–118, 1981. doi:10.1103/PhysRevLett.46.115.

[8] A Meige. One-dimensional particle-in-cell simulation of a current-free double layer in an expanding plasma. *Phys. Plasmas*, 12(5):052317, 2005. doi:10.1063/1.1897390.

[9] K Goswami. Theory of current-free double layers in plasmas. *Phys. Plasmas*, 15(6):062111, 2008. doi:10.1063/1.2937153.

[10] G Hairapetian. Observation of a stationary, current-free double-layer in a plasma. *Phys. Rev. Lett.*, 65(2):175–178, 1990. doi:10.1103/PhysRevLett.65.175.

[11] C Charles. Current-free double-layer formation in a high-density helicon discharge. *Appl. Phys. Lett.*, 82(9):1356–1358, 2003. doi:10.1063/1.1557319.

[12] S. A. Cohen, N. S. Siefert, S. Stange, R. F. Boivin, E. E. Scime, and F. M. Levinton. Ion acceleration in plasmas emerging from a helicon-heated magnetic-mirror device. *Phys. Plasmas*, 10(6):2593–2598, 2003. doi:10.1063/1.1568342.

[13] O Sutherland. Experimental evidence of a double layer in a large volume helicon reactor. *Phys. Rev. Lett.*, 95(20):205002–4, 2005. doi:10.1103/PhysRevLett.95.205002.

[14] A Keesee. The ion velocity distribution function in a current-free double layer. *Phys. Plasmas*, 12(9):093502, 2005. doi:10.1063/1.2033647.

[15] N. Plihon, P. Chabert, and C. S. Corr. Experimental investigation of double layers in expanding plasmas. *Phys. Plasmas*, 14(1):013506, 2007. doi:10.1063/1.2424429.

[16] K Takahashi. Ion acceleration in a solenoid-free plasma expanded by permanent magnets. *Phys. Plasmas*, 15(8):084501, 2008. doi:10.1063/1.2965497.

[17] H S Byhring, C Charles, Å Fredriksen, and R W Boswell. Double layer in an expanding plasma: Simultaneous upstream and downstream measurements. *Phys. Plasmas*, 15(10):102113, 2008. doi:10.1063/1.3002396.

[18] C Charles. A review of recent laboratory double layer experiments. *Plasma Sources Sci. Technol*, 16(4):R1–R25, 2007. doi:10.1088/0963-0252/16/4/R01.

[19] C Charles. An experimental investigation of alternative propellants for the helicon double layer thruster. *J. Phys. D: Appl. Phys.*, 41(17):175213, 2008. doi:10.1088/0022-3727/41/17/175213.

[20] C Charles, R W Boswell, W Cox, R Laine, and P MacLellan. Magnetic steering of a helicon double layer thruster. *Appl. Phys. Lett.*, 93(20):201501, 2008. doi:10.1063/1.3033201.

[21] M D West. High density mode in xenon produced by a helicon double layer thruster. *J. Phys. D: Appl. Phys.*, 42(24):245201, 2009. doi:10.1088/0022-3727/42/24/245201.

[22] C Franck. Transition from unbounded to bounded plasma whistler wave dispersion. *Phys. Plasmas*, 9(8):3254–3258, 2002. doi:10.1063/1.1494069.

[23] T. Windisch, K. Rahbarnia, O. Grulke, and T. Klinger. Study of a scalable large-area radio-frequency helicon plasma source. *Plasma Sources Sci. Technol.*, 19(5):055002, October 2010. doi:10.1088/0963-0252/19/5/055002.

[24] C Franck. Mode transitions in helicon discharges. *Phys. Plasmas*, 10(1):323–325, 2003. doi:10.1063/1.1528903.

[25] T Lafleur. Detailed plasma potential measurements in a radio-frequency expanding plasma obtained from various electrostatic probes. *Phys. Plasmas*, 16(4):044510, 2009. doi:10.1063/1.3125314.

[26] I Sudit. Rf compensated probes for high-density discharges. *Plasma Sources Sci. Technol.*, 3(2):162–168, 1994. doi:10.1088/0963-0252/3/2/006.

[27] M. A. Lieberman, C. Charles, and R. W. Boswell. A theory for formation of a low pressure, current-free double layer. *Journal of Physics D-applied Physics*, 39(15):3294–3304, August 2006. doi:10.1088/0022-3727/39/15/011.